AJNR

Quantitative Differentiation Between Healthy and Disordered Brain Matter in Patients with Neurofibromatosis Type I Using Diffusion Tensor Imaging

S.J.P.M. van Engelen, L.C. Krab, H.A. Moll, A. de Goede-Bolder, S.M.F. Pluijm, C.E. Catsman-Berrevoets, Y. Elgersma and M.H. Lequin

AJNR Am J Neuroradiol 2008, 29 (4) 816-822
doi: https://doi.org/10.3174/ajnr.A0921
http://www.ajnr.org/content/29/4/816

ORIGINAL RESEARCH

Quantitative Differentiation Between Healthy and Disordered Brain Matter in Patients with Neurofibromatosis Type I Using Diffusion Tensor Imaging

S.J.P.M. van Engelen
L.C. Krab
H.A. Moll
A. de Goede-Bolder
S.M.F. Pluijm
C.E. Catsman-Berrevoets
Y. Elgersma
M.H. Lequin

BACKGROUND AND PURPOSE: Hyperintensities on T2-weighted images are seen in the brains of most patients with neurofibromatosis type I (NF-1), but the origin of these unidentified bright objects (UBOs) remains obscure. In the current study, we examined the diffusion characteristics of brain tissue in children with NF-1 to test the hypothesis that a microstructural abnormality is present in NF-1.

MATERIALS AND METHODS: Diffusion tensor imaging (DTI) was performed in 50 children with NF-1 and 8 controls. Circular regions of interest were manually placed in 7 standardized locations in both hemispheres, including UBO sites. Apparent diffusion coefficients (ADC), fractional anisotropy (FA), and axial anisotropy (A_m) were used to differentiate quantitatively between healthy and disordered brain matter. Differences in eigenvalues (λ_1, λ_2, λ_3) were determined to examine parenchymal integrity.

RESULTS: We found higher ADC values for UBOs than for normal-appearing sites ($P < .01$) and higher ADC values for normal-appearing sites than for controls ($P < .04$ in 5 of 7 regions). In most regions, we found no differences in FA or A_m. Eigenvalues λ_2 and λ_3 were higher at UBO sites than in normal-appearing sites ($P < .04$).

CONCLUSION: With ADC, it was possible to differentiate quantitatively between normal- and abnormal-appearing brain matter in NF-1 and also between normal-appearing brain matter in NF-1 and healthy brain matter in controls, indicating subtle pathologic damage disrupting the tissue microstructure in the NF-1 brain. Higher diffusivity for λ_1, λ_2, and λ_3 indicates that this disturbance of microstructure is caused by accumulation of fluid or vacuolation.

Hyperintensities on T2-weighted images are seen in the brains of most patients with neurofibromatosis type I (NF-1). Although many imaging techniques have been used to assess these unidentified bright objects (UBOs), their origin remains obscure.[1-4] The only pathologic study performed in NF-1 so far revealed intramyelinic vacuolar changes or spongiotic myelinopathy that correlated with the hyperintensities found on T2-weighted images.[5] In addition to conventional MR imaging, several studies have used diffusion-weighted imaging (DWI) with assessment of apparent diffusion coefficients (ADCs) to gain information on UBOs that cannot be assessed by inspection of conventional images alone. On the basis of the high ADC values, a widespread myelin disorder was suggested to be present in patients with NF-1.[6-9] However, ADC reflects only the magnitude of the diffusion of water molecules. Although high ADC values might suggest increased water content of the brain, with ADC alone, it is not possible to examine the microstructural integrity of the parenchyma. Diffusion tensor imaging (DTI), which measures the degree and direction of molecular diffusivity, is able to detect white matter abnormalities and characterize them in terms of white matter fiber integrity.[10,11]

DTI generates a diffusion tensor matrix from a series of DWIs. By matrix diagonalization, the 3 eigenvalues λ_1, λ_2, and λ_3 can be calculated. λ_1 has the largest value and reflects the diffusivity parallel to a structure; λ_2 and λ_3 are the middle and smallest eigenvalues, respectively; and their average represents the diffusivity perpendicular to a structure. Various anisotropy indexes (fractional anisotropy [FA], axial anisotropy [A_m]) can be calculated by using the eigenvalues. They describe the ratio of the eigenvalues and are scaled from zero (isotropic) to 1 (anisotropic) and reflect the microstructure of white matter tracts. Looking at the eigenvalues themselves enables specific assessment of myelin integrity, as distinct from axonal integrity.[12,13] Recently, a DTI study on adult patients with NF-1 revealed higher ADC and lower FA values. Unfortunately, changes in eigenvalues were not reported.[14]

The purpose of this study was to examine the diffusion characteristics of brain tissue in children with NF-1 by means of DTI and to test the hypothesis that a microstructural abnormality is present in NF-1. We tested this in 3 ways: First, by assessing ADC and indexes of anisotropic diffusion, we tried to differentiate quantitatively between normal- and abnormal-appearing brain tissue in children with NF-1. Second, we examined the normal-appearing parenchyma in NF-1 to see if it is different from parenchyma in healthy controls. Third, we looked at parenchymal integrity at UBO sites and normal-

Received August 16, 2007; accepted after revision October 24.

From the Departments of Pediatric Radiology (S.J.P.M.v.E., M.H.L.), General Paediatrics (L.C.K., H.A.M., A.d.G.-B.), Neuroscience (L.C.K., Y.E.), Public Health (S.M.F.P.), and Pediatric Neurology (C.E.C.-B.), The NF-1 CoRe Team (Cognitive Research Team), Erasmus MC-Sophia Children's Hospital, Rotterdam, the Netherlands.

This work was supported by grants from the Dutch association for brain research (Hersenstichting Nederland), the Sophia Children's Hospital Fund, and Erasmus MC.

Paper previously presented in part at: European Congress of Radiology, March 9–13, 2007; Vienna, Austria (7-minute oral presentation); and European Society of Pediatric Radiology, June 4–8, 2007; Barcelona, Spain (3-minute oral presentation).

Please address correspondence to Maarten H. Lequin, MD, PhD, Department of Pediatric Radiology, Erasmus MC-Sophia Children's Hospital, Dr. Molewaterplein 60, 3015 GJ Rotterdam, the Netherlands; e-mail: m.lequin@erasmusmc.nl

DOI 10.3174/ajnr.A0921

appearing sites by assessment of the eigenvalues. In addition, because T2-weighted hyperintensities in the hippocampus have been suggested to have a different pathogenetic basis from classic UBOs,[15] we paid special attention to the diffusion characteristics of the hippocampal hyperintensities to see if they were different from those in other regions of interest.

Materials and Methods

Subjects

Data for this study were obtained in the context of a larger study on NF-1 and cognitive functioning. All participants were recruited from the multidisciplinary NF-1 outpatient clinic of the hospital. Inclusion criteria were the following: 8–17 years of age, NF-1 diagnosis according to the criteria of the National Institutes of Health,[16] and informed consent from parents and children older than 12 years of age. Exclusion criteria were the following: segmental NF-1 (because brain involvement is not certain in these patients), pathology of the central nervous system (CNS) (other than asymptomatic gliomas), deafness, severe impaired vision, use of antiepileptics, inefficient production and comprehension of the Dutch language, and severe mental retardation (intelligence quotient <48).

One hundred twenty-six children fulfilled the age criterion. Twelve children were excluded on the basis of possible segmental NF-1 ($n = 3$), the use of antiepileptics ($n = 3$), hydrocephalus ($n = 3$), severe mental retardation ($n = 1$), and inefficient production and comprehension of the Dutch language ($n = 2$). The remaining 114 children were invited to participate in the larger study, of which 62 consented. The study was approved by the medical ethics committee of our institution. A total of 50 of 62 children who participated in the larger study consented to MR imaging examination (21 girls; mean age, 12.2 years; range, 8.1–15.7 years; and 29 boys, mean age, 12.3 years; range, 8.0–16.5 years).

Image Acquisition

MR anatomic imaging with DTI was performed by using a 1.5T system (EchoSpeed; GE Healthcare, Milwaukee, Wis) and a dedicated 8-channel head coil. DTI data were acquired by using a multi-repetition single-shot echo-planar sequence with a section thickness of 3 mm with no gap. The DTI images were obtained in 25 gradient directions with a sensitivity of $b = 1000$ s/mm^2, TR = 15,000 ms, TE = 82.1 ms, 1 average, FOV of 240 × 240 mm^2, and a matrix of 128 × 128 resulting in a voxel size of 1.8 × 1.8 × 3.0 mm^3. Acquisition time was 5:28 minutes with a total of 53 sections to cover the entire brain.

Data Collection

All images were analyzed by visual inspection by an experienced pediatric neuroradiologist to exclude CNS tumors. Hyperintense lesions on T2-weighted, fluid-attenuated inversion recovery (FLAIR), and diffusion images ($b = 0$ s/mm^2) were classified as UBOs. When no hyperintense lesion was present, the area was scored as a normal-appearing site.

For quantitative data analysis, ADC, FA, and A_m, and eigenvalues were used. FA measures the fraction of the magnitude of the diffusion tensor that can be ascribed to anisotropic diffusion.[17] A_m reflects the shape of the diffusion ellipsoid.[18] ADC, FA, and eigenvalue maps were reconstructed by using commercially available software (Functool 3.1.23, Advanced Workstation 4.1; GE Healthcare). Circular regions of interest of specific sizes were manually placed in 7 predetermined anatomic locations in both hemispheres: the cerebral peduncle (CP), cerebellar white matter (CWM), hippocampus (HI), thalamus (TH), globus pallidus (GP), and frontal (FWM) and parieto-occipital (POWM) white matter. The size of the regions of interest was 100 mm^2 for CWM; 70 mm^2 for CP; 170 mm^2 for HI, POWM, and FWM; and 130 mm^2 for GP and TH, according to the method of Alkan et al (Fig 1).[8] All region-of-interest placement was done on the $b = 0$ s/mm^2 images because anatomic detail was better on these images than on the computed maps, ensuring anatomic precision. Regions of interest were automatically superimposed on the functional maps by the software that was used in this study. ADC maps were used to exclude CSF from measurements to minimize overestimation of the ADC values. FA maps were used when placing regions of interest in the GP and TH region to avoid as much as possible the involvement of the corticospinal tract (anterior and posterior limb of the internal capsula).

Statistical Analysis

For statistical analysis ADC, FA, and eigenvalues calculated by the software were used. A_m values were calculated by using the eigenvalues λ_1, λ_2, and λ_3 in the following way:

$$A_m = \frac{\lambda_1 - \frac{1}{2}(\lambda_2 + \lambda_3)}{\lambda_1 + \lambda_2 + \lambda_3}.$$

To determine intraobserver reliability of region-of-interest placement, the same observer repeated the placement in a subset of 10 scans. Single-measure intraclass correlation coefficients (ICCs) were calculated to compare the variability of data obtained.

To explore mean group differences, we averaged values obtained of the left and right hemisphere per region, per subject. All regions were then divided into the following groups on the basis of NF-1 and on the prevalence of UBOs: 1) NF-1 regions with bilateral UBOs or with a UBO on 1 site and a normal-appearing contralateral site, 2) NF-1 regions with no UBOs (both sites normal-appearing), and 3) healthy controls. Differences in ADC, FA, A_m, and eigenvalues were compared by using 1-way analysis of variance or the Kruskal-Wallis test (if the distribution of the data was skewed). Significance was set at $P < .05$, and post hoc comparisons were done by using the Scheffé test. Differences in the proportions of λ_1 and λ_2, as well as the proportions of λ_1 and λ_3, between HI hyperintensities and UBOs in other regions, were analyzed by using the Wilcoxon signed rank test for nonparametric related samples. Statistical analysis was done by using the Statistical Package for the Social Sciences 10.0 for Windows (SPSS, Chicago, Ill).

Results

Intraobserver Reliability of Region-of-Interest Placement

Reproducibility of region-of-interest placement by a single observer proved moderate to very good, with ICCs between 0.47 and 0.91. The lowest values were found for the GP (left hemisphere, 0.47; right hemisphere, 0.70), HI (left, 0.66; right, 0.55), and TH (left, 0.52; right, 0.73), whereas the highest ICCs were found for CWM (left, 0.67; right, 0.91). However, the wide range of ICCs in these regions is disconcerting. In FWM, POWM, and CP, the ICC was >0.71.

Qualitative Evaluation of UBOs

Controls (4 girls; age range, 7.4–12.1 years; mean age, 10.8 years; and 4 boys; age range, 7.8–12.0 years; mean age, 9.6 years) were selected for comparison. All controls were without chronic disease and had normal findings on MR imaging.

Sixty-eight percent of the children with NF-1 ($n = 34$) were

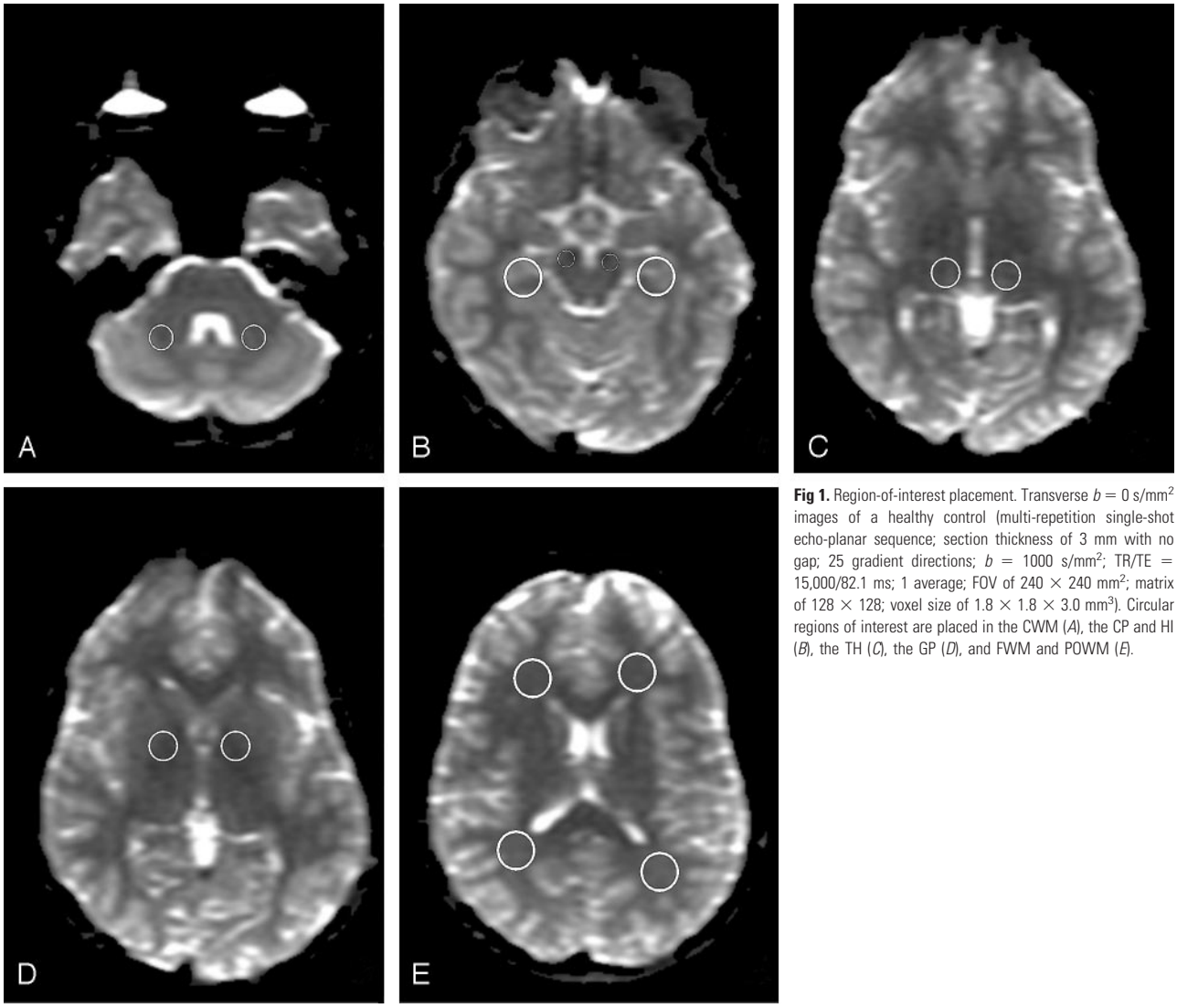

Fig 1. Region-of-interest placement. Transverse $b = 0$ s/mm^2 images of a healthy control (multi-repetition single-shot echo-planar sequence; section thickness of 3 mm with no gap; 25 gradient directions; $b = 1000$ s/mm^2; TR/TE = 15,000/82.1 ms; 1 average; FOV of 240 × 240 mm^2; matrix of 128 × 128; voxel size of 1.8 × 1.8 × 3.0 mm^3). Circular regions of interest are placed in the CWM (*A*), the CP and HI (*B*), the TH (*C*), the GP (*D*), and FWM and POWM (*E*).

found to have UBOs in 1 or more of the 7 selected regions, which could be detected and measured on the $b = 0$ s/mm^2 images. Forty-six percent of the children with NF-1 had UBOs in the GP (13 bilateral, 10 unilateral), 14% in the TH (2 bilateral, 5 unilateral), 50% in the CWM (16 bilateral, 9 unilateral), and 22% in the CP (9 bilateral, 7 unilateral). The HI was visually scored bilaterally hyperintense on T2- and FLAIR images in 48% of the children with NF-1. No circumscript UBOs were found in POWM and FWM. Figure 2 presents ADC, FA, and eigenvalues maps of a girl with NF-1 with a UBO in the left GP and a normal-appearing contralateral side.

Measurements in the CP could not be performed in 2 children with NF-1; and in 1 of those children, motion artifacts also prohibited measurements in the HI. Mean ± SD of ADC, FA, A_m, and eigenvalues per region per group are plotted in Figs 3–6.

Quantitative Differentiation of Healthy and Disordered Brain Matter in NF-1

ADC values were significantly higher in regions where UBOs were present than in the matching regions with no UBOs (for all regions, $P < .01$). Also, ADC values were higher in NF-1 regions with no UBOs than in the regions of healthy controls, significantly so in the POWM and CWM ($P < .03$), FWM ($P < .01$), GP ($P < .04$), and TH ($P < .01$; Fig 3). To investigate the influence of region-of-interest size, we performed additional measurements in the GP region in a subset of 15 patients, by using a circular region of interest of 30 mm^2. This smaller region-of-interest size resulted in a significantly higher ADC value ($P < .01$) as compared with the value obtained by a region of interest of 130 mm^2.

With respect to FA values, the results were not as clear-cut. Although there was a trend toward FA values in NF-1 regions, with UBOs being lower than those in matching NF-1 regions without UBOs and controls, these differences were not significant for most regions (Fig 4). Only for CWM was the FA value in NF-1 with UBOs significantly lower than that in NF-1 without UBOs ($P < .01$). Remarkably, results in the GP were opposite to those in other tissues, with higher FA values for NF-1 with UBOs as compared with NF-1 without UBOs ($P < .01$).

A_m values were lower in NF-1 regions with UBOs as compared with NF regions without UBOs, significantly so in CWM ($P < .02$) and CP ($P < .01$). In addition, A_m values were also significantly lower in NF-1 regions without UBOs as compared with controls in the TH ($P < .02$). In GP, an opposite trend was shown: The value found for NF-1 with UBOs was

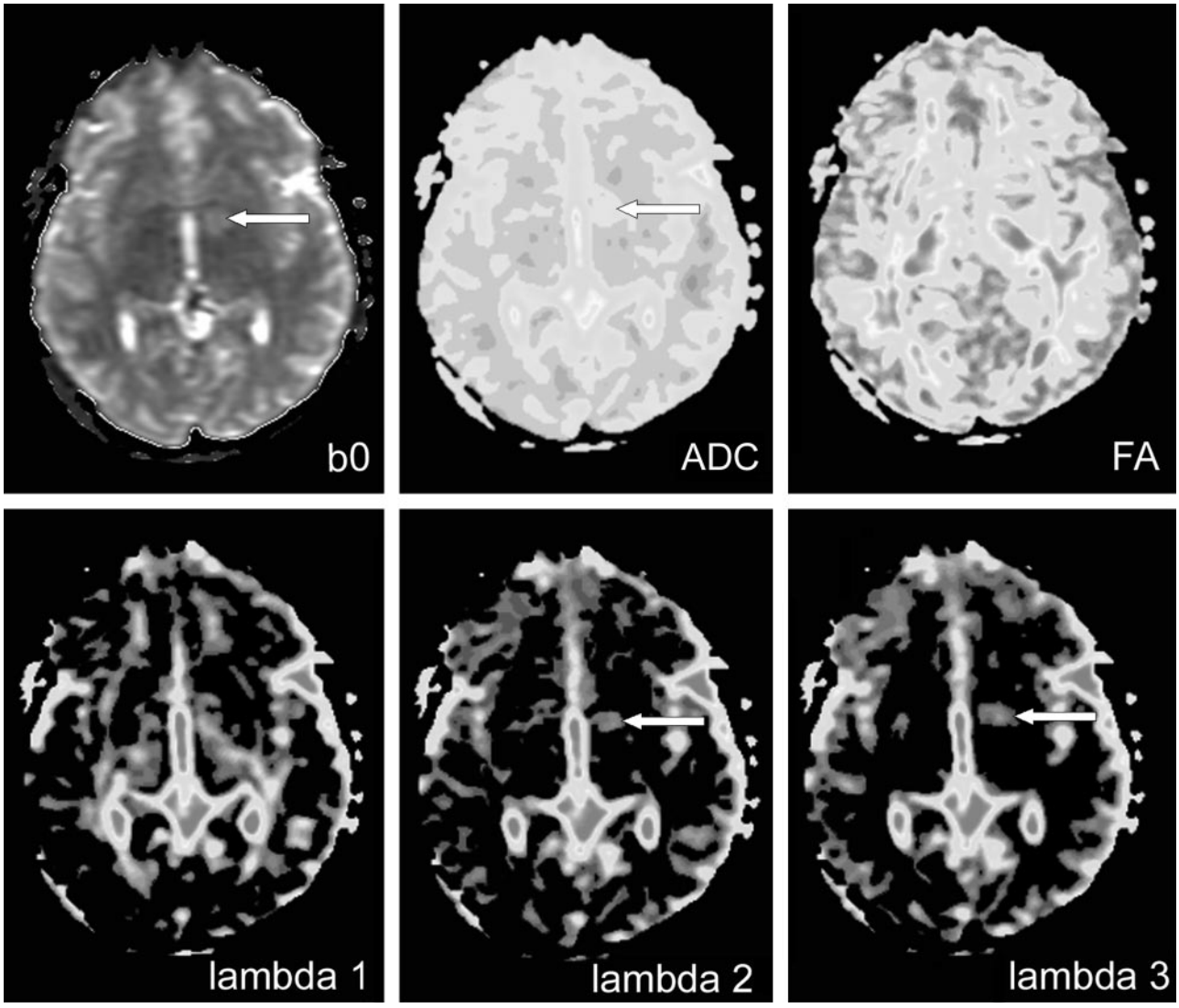

Fig 2. DTIs of the globus pallidus. Transverse DTIs (multi-repetition single-shot echo-planar sequence; section thickness of 3 mm with no gap; 25 gradient directions; $b = 1000$ s/mm^2; TR/TE = 15,000/82.1 ms; 1 average; FOV of 240 × 240 mm^2; matrix of 128 × 128; voxel size of 1.8 × 1.8 × 3.0 mm^3). Girl with NF-1 (13 years of age) with a unilateral UBO in the GP. Arrow indicates an area of high intensity on the $b = 0$ s/mm^2 image and high values on the ADC, λ_2 (lambda 2), and λ_3 (lambda 3) maps.

significantly higher as compared with that of NF-1 without UBOs ($P < .01$). No significant differences in A_m were found between UBO, normal-appearing sites, and controls in the other regions assessed (Fig 5).

Microstructural Integrity of NF-1 Brains

To examine microstructural integrity of the brain parenchyma in NF-1, we assessed the eigenvalues (Table). In all regions tested, NF-1 regions with UBOs had eigenvalues higher than those of NF-1 regions without UBOs (Fig 6). In CWM and GP, all 3 eigenvalues were significantly higher ($P < .02$); in HI, CP, and TH, λ_2 and λ_3 were significantly higher ($P < .04$), indicating a loss of microstructure of the brain parenchyma in children with NF-1 with UBOs.

The eigenvalues in NF-1 regions without UBOs closely followed those in healthy controls, indicating that the microstructure is close to normal in children without UBOs, even though some slight but significant elevations were seen (FWM, $P < .01$ for λ_1 and λ_2; HI, $P < .02$ for λ_1). The exception is in the TH, where the eigenvalues of NF-1 without UBOs were much higher than those of healthy controls, significantly so for λ_2 and λ_3 ($P < .01$).

Analysis of the difference in proportions of λ_1 and λ_2 for hyperintensities in the HI and for UBOs in other regions revealed that there were no differences in the proportions of λ_1-λ_2 for HI compared with the TH ($P < .11$) or GP ($P < .59$). The same results were found for the differences in the proportions of λ_1 and λ_3. This indicates that the diffusion perpendicular to the axon for HI is not different from other gray matter areas like the TH and GP. Compared with white matter areas CP and CWM, there were significantly different proportions for λ_1-λ_2 ($P < .02$ and $P < .01$).

Discussion

DTI in 50 children with NF-1 and 8 controls revealed significantly higher ADC values in NF-1 regions with UBOs as compared with NF-1 regions without UBOs and in NF-1 regions without UBOs as compared with controls. ADC values reflect the overall brain water content[19]; thus the differences between NF-1 regions with UBOs, NF-1 regions without UBOs, and

DTI values per ROI*

ROI	Group	No.	Mean Value					
			ADC $\times 10^{-3}$ mm^2/s	FA	$\lambda_1 \times 10^{-3}$ mm^2/s	$\lambda_2 \times 10^{-3}$ mm^2/s	$\lambda_3 \times 10^{-3}$ mm^2/s	A_m
POWM	NAS	50	0.79 ± 0.05	0.31 ± 0.06	1.09 ± 0.06	0.74 ± 0.06	0.52 ± 0.07	0.20 ± 0.04
	Controls	8	0.75 ± 0.02	0.36 ± 0.06	1.06 ± 0.04	0.70 ± 0.05	0.48 ± 0.03	0.19 ± 0.06
FWM	NAS	50	0.80 ± 0.04	0.31 ± 0.04	1.04 ± 0.05	0.76 ± 0.04	0.56 ± 0.05	0.16 ± 0.02
	Controls	8	0.75 ± 0.03	0.30 ± 0.02	0.98 ± 0.04	0.71 ± 0.04	0.53 ± 0.04	0.16 ± 0.02
GP†	UBO	23	0.83 ± 0.07	0.25 ± 0.06	1.02 ± 0.12	0.79 ± 0.07	0.64 ± 0.06	0.13 ± 0.04
	NAS	27	0.72 ± 0.04	0.17 ± 0.04	0.83 ± 0.05	0.70 ± 0.04	0.60 ± 0.04	0.09 ± 0.01
	Controls	8	0.70 ± 0.02	0.16 ± 0.02	0.81 ± 0.03	0.68 ± 0.03	0.58 ± 0.03	0.08 ± 0.02
TH	UBO	7	0.81 ± 0.04	0.29 ± 0.10	1.04 ± 0.05	0.75 ± 0.06	0.61 ± 0.08	0.15 ± 0.04
	NAS	43	0.76 ± 0.03	0.31 ± 0.05	1.02 ± 0.05	0.70 ± 0.04	0.55 ± 0.04	0.17 ± 0.03
	Controls	8	0.70 ± 0.02	0.36 ± 0.06	0.98 ± 0.07	0.63 ± 0.03	0.47 ± 0.02	0.21 ± 0.04
HI	UBO	23	0.90 ± 0.05	0.20 ± 0.04	1.07 ± 0.51	0.87 ± 0.42	0.72 ± 0.51	0.10 ± 0.03
	NAS	25	0.84 ± 0.04	0.21 ± 0.04	1.04 ± 0.07	0.82 ± 0.04	0.66 ± 0.04	0.12 ± 0.03
	Controls	8	0.80 ± 0.02	0.21 ± 0.02	0.97 ± 0.02	0.78 ± 0.03	0.63 ± 0.03	0.11 ± 0.02
CWM†	UBO	25	0.85 ± 0.14	0.32 ± 0.11	1.11 ± 0.08	0.85 ± 0.35	0.61 ± 0.13	0.20 ± 0.18
	NAS	25	0.72 ± 0.06	0.43 ± 0.11	1.05 ± 0.13	0.65 ± 0.07	0.47 ± 0.09	0.23 ± 0.07
	Controls	8	0.68 ± 0.02	0.45 ± 0.08	1.00 ± 0.06	0.62 ± 0.05	0.43 ± 0.04	0.23 ± 0.05
CP	UBO	16	0.89 ± 0.05	0.44 ± 0.06	1.31 ± 0.09	0.77 ± 0.09	0.54 ± 0.09	0.25 ± 0.04
	NAS	33	0.81 ± 0.05	0.47 ± 0.05	1.32 ± 0.11	0.69 ± 0.09	0.47 ± 0.05	0.30 ± 0.05
	Controls	8	0.80 ± 0.05	0.51 ± 0.04	1.32 ± 0.12	0.63 ± 0.05	0.43 ± 0.04	0.33 ± 0.03

Note:—ROI indicates region of interest; NAS, normal-appearing sites; POWM, parieto-occipital white matter; FWM, frontal white matter; GP, globus pallidus; TH, thalamus; HI, hippocampus; CWM, cerebellar white matter; CP, cerebral peduncle; UBO, unidentified bright object; ADC, apparent diffusion coefficient; FA, fractional anisotropy; A_m, axial anisotropy.
* Values are averaged for left and right hemispheres. For all indices, mean values ± SD are given for regions with UBOs, regions without UBOs (NAS), and healthy controls.
† Nonparametric data.

controls found in this study can primarily be explained by increased water content of the brain parenchyma in NF-1, which is apparently exacerbated in NF-1 regions with UBOs. These findings confirm those of previous reports.[6-9,14] However, the ADC values found in this study are not as high as the ADC values found previously. An explanation of lower ADC values may be found in the shorter effective TE and the different b-value that were used in our scanning protocol compared with reported DWI protocols.[20] Also DTI improves the ability to avoid partial volume effects of CSF by fine-tuning the region of interest placement by simultaneous use of $b = 0$ s/mm^2 images, ADC, and FA maps. Another important technical issue is the chosen size of the region of interest because it influences the ADC values. Larger regions of interest result in lower ADC values because the value represents an average of more voxels, the area of the UBO and surrounding tissue, as demonstrated in the GP by the subtest in which a region of interest of 30 mm^2 instead of 130 mm^2 was used.

DTI may facilitate a better understanding of the abnormalities seen in NF-1 because evaluation of microstructural integrity of the parenchyma can be achieved by assessing anisotropy indexes and eigenvalues. Anisotropy can be influenced by factors such as axon packing, relative membrane permeability to water, internal axon structure, myelination, and tissue water content.[21] ADC values in this study were higher in NF-1 regions with UBOs and in NF-1 regions without UBOs than in healthy controls, suggesting increased tissue water content or decreased axon packing. However, on the basis of FA values in our study, it was only possible to differentiate between NF-1 regions with UBOs and NF-1 regions without UBOs in the CWM and GP. Remarkably, in the latter, we found higher FA values for NF-1 with UBOs as compared with NF-1 without UBOs and controls, which is a counterintuitive finding.

When carefully re-examining region-of-interest placements in the GP, we realized that it is almost impossible to avoid partial volume effects of the posterior limb of the internal capsula, even when regions of interest are drawn smaller (30 mm^2 instead of 130 mm^2). UBOs are typically found very near or in some cases in the internal capsula. The high anisotropy of the internal capsula affects the measured FA values for the GP. Low ICC and high variability (Fig 3) also show the difficulties of taking measurements in the GP region. In contrast to our results in children with NF-1, a recently published study on adult patients with NF-1 by using DTI found significantly lower FA values in NF-1 brains than in healthy brains, indicating generalized microstructural alterations and dysmyelination in adult patients with NF-1.[14] A caveat of the study in adult patients is that it did not assess alterations of the eigenvalues, and it is, therefore, not possible to relate changes in FA to dysmyelination. Lower FA values at UBO sites might also be caused by damage to the axon as shown by MR spectroscopy.[22] The study in adult patients found severely reduced concentrations of *N*-acetylaspartate at UBO sites, indicating that an increased myelin turnover was present, which could lead to subsequent axonal damage in adult patients with NF-1. We found no evidence for axonal damage in children with NF-1, which might be an explanation of why we did not find lowered FA values in our study.

We also did not find differences in the shape of the diffusion ellipsoid, when looking at A_m values, between children with NF-1 with or without UBOs or healthy controls in most regions of interest. Although of all anisotropy indexes, A_m shows the strongest trend in relative changes,[23] in this study, A_m was only slightly more sensitive than FA. The homogeneous attenuated white matter structures in CWM and CP in contrast to GP, TH, and HI, where the tissue also contains gray matter, which has zero anisotropy,[24] could be the reason why we did find differences in anisotropy in CWM and CP between NF-1 with UBOs and NF-1 without UBOs, but not in the other regions of interest. If the eigenvalues λ_1 and λ_2 and/or λ_3

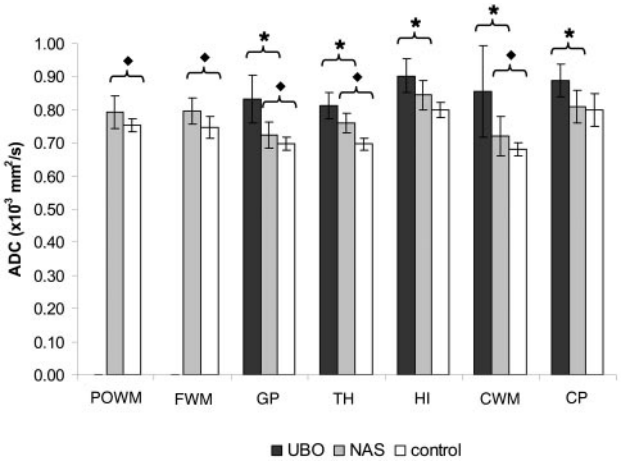

Fig 3. Mean ADC values. The cohort is divided in 3 groups: NF-1 regions with UBOs (UBO), NF-1 regions with normal-appearing brain matter (NAS), and controls. Mean ADC values for UBOs are higher than those for NAS in all regions (except POWM and FWM where no UBOs were found). Mean ADC values for NAS are significantly higher than those of controls in all regions, except CP. For convenience, the results of the HI area are presented in the same figure as the results of the other regions of interest. HI hyperintensities are presented as UBOs and normal-appearing HI areas as NAS. Significant differences between UBO and NAS are indicated by ★ and between NAS and controls by ◆.

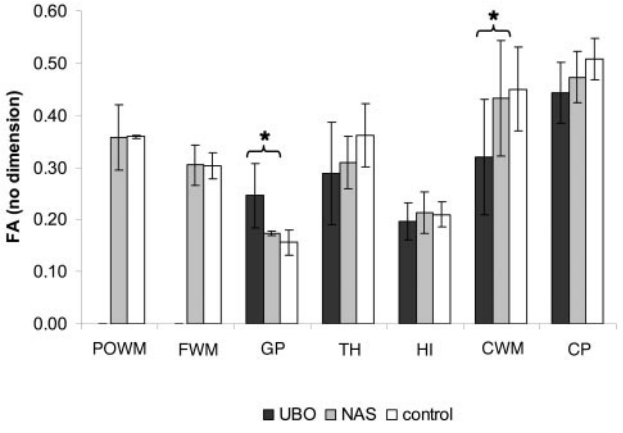

Fig 4. FA values. Mean FA values ± SD for UBO, normal-appearing sites (NAS), and controls are plotted for the 7 regions of interest. Few significant differences are found between UBO and NAS, indicated by ★.

changed in the same direction, as found in our study, no differences in FA and A_m would be observed (but the change in ADC would be marked).[25]

Higher eigenvalues in NF-1 regions with UBOs indicate that the microstructure of the parenchyma is different from the parenchyma in NF-1 regions without UBOs. Animal studies have shown that an increment of axial diffusivity (λ_2 and λ_3) is related to myelin deficiency, whereas a decrease of parallel diffusivity (λ_1) indicates axonal disturbance.[26-28] Our findings of higher values for λ_2 and λ_3 indicate that diffusion perpendicular to the white matter structure is higher. Because we did not find lower values for λ_1 in NF-1 regions with UBOs than in NF-1 regions without UBOs, we hypothesize that the observed changes of the brain tissue in NF-1 are not caused by damage to the axon, but relate to myelin deficiency. The higher value for all eigenvalues in our study, especially for λ_1, has not previously been reported in human or animal studies. Accumulation of fluid hypothetically should increase the magnitude of all 3 eigenvalues from their normal values.[29] Our

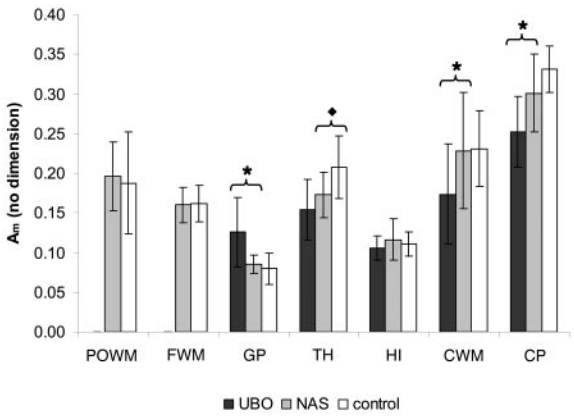

Fig 5. A_m values. Mean A_m values ± SD for UBO, normal-appearing sites (NAS), and controls per regions of interest. Significant differences between UBO and NAS are indicated by ★ and between NAS and controls by ◆.

study, therefore, indicates intramyelinic edema or vacuolar changes in the myelin. This confirms the study of DiPaolo et al,[5] which was the only pathologic study performed in NF-1. Autopsy and histopathologic examination performed on 3 patients with NF-1 revealed intramyelinic vacuolar changes or spongiotic myelinopathy that correlated with the hyperintensities found on T2-weighted images. No stainable material was found within the vacuoles, which suggests that in life, they are filled with water.[5]

Notably, our study is not a radiology-pathology correlation study. To our knowledge, the specificity of changes of eigenvalues due to myelin disturbance in humans has not been tested. Because we were not able to perform histopathologic examinations in our cohort, no proof can be provided for the suggestion of myelin deficiency or vacuolar changes, however likely that eigenvalues will allow an assessment of myelin.

HI hyperintensities were of special interest in our study because a different pathogenetic basis from classic UBOs was suggested.[15] Impairments in learning and behavior in mouse models of NF-1 are thought to be suggestive of disordered hippocampal functioning.[15] We measured DTI parameters to examine if there is an underlying microstructural change in the hippocampal region distinct from other regions of interest. We found higher ADC values in hyperintense-appearing hippocampal areas than in normal-appearing hippocampal areas, which could explain disordered hippocampal functioning, but no differences in FA and A_m. Although anisotropy indices in HI were lower compared with other regions of interest, eigenvalues showed no different pattern when comparing HI with other gray matter structures like GP and TH. Therefore, distinct pathogenesis between hyperintense HI and classic UBOs cannot be concluded in this study by using DTI parameters.

Our study has several limitations such as a limited number of children with NF-1 with and without UBOs and an even smaller number of control subjects. However, post hoc power analyses showed that power was >0.80 for all analyses in which children with NF-1 with and without UBOs were compared with healthy controls for ADC values. Although our findings contribute to the unraveling of UBOs, for we have been able to prove that the high ADC values in UBOs observed in previous publications are due to increased axial diffusivity,

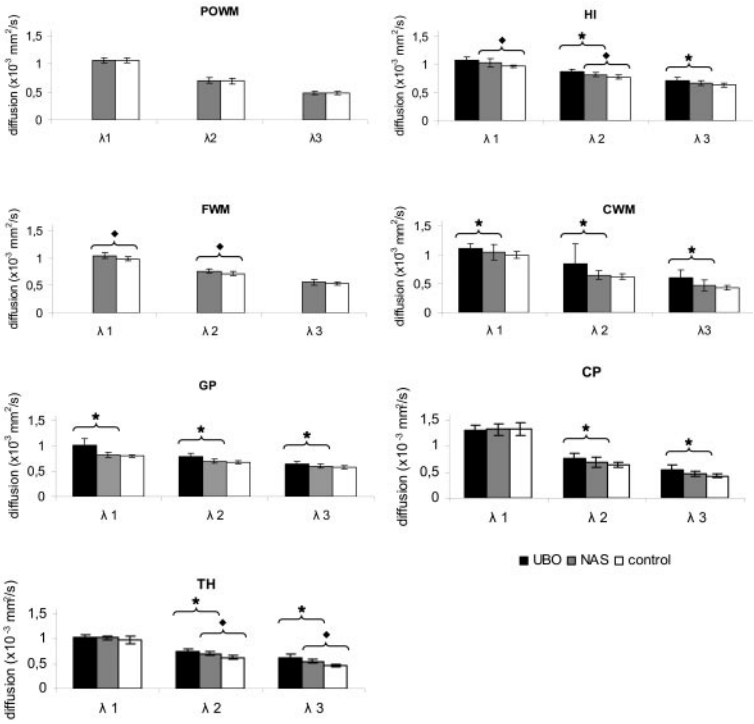

Fig 6. Eigenvalues per region. For UBO, normal-appearing sites (NAS), and controls, mean values for the 3 eigenvalues are plotted for each region. In all regions where UBOs are found, λ_1, λ_2, and λ_3 are higher for UBOs than for NAS and higher for NAS compared with controls. Significant differences between UBO and NAS are indicated by ★ and between NAS and controls by ◆.

no histologic correlation with the observed diffusion signal-intensity abnormalities in NF-1 could be provided.

Conclusion

On the basis of the results obtained in the current study, it can be concluded that it is possible to quantitatively differentiate between healthy and disordered brain parenchyma in children with NF-1 by using ADC values. Although no differences were found in anisotropy indexes, higher values for λ_2 and λ_3 in NF-1 regions with UBOs than in NF-1 regions without UBOs indicate higher axial diffusivity because of less obstruction (presumably due to water accumulation in myelin). The higher λ_1 contradicts axonal disturbance. The observed high diffusivity for all 3 eigenvalues (λ_1, λ_2, and λ_3) in NF-1 regions with UBOs, as compared with NF-1 regions without UBOs and controls, supports pathologic findings and could be explained by a disturbed microstructure of the NF-1 brain due to accumulation of fluid or vacuolation when UBOs are present. A distinct pathogenesis between hyperintense HI and classic UBOs was not found in this study by using DTI parameters.

Acknowledgments

We thank all children and their parents for their participation, all technicians who performed MR imaging, and the representatives of the NF-1 clinical workgroup in the departments of pediatric dermatology, pediatric ophthalmology, general pediatrics, pediatric neurology, and clinical genetics.

References

1. Huson SM, Compston DA, Harper PS, et al. **A genetic study of von Recklinghausen neurofibromatosis in south east Wales. I. Prevalence, fitness, mutation rate, and effect of parental transmission on severity.** *J Med Genet* 1989;26:704–11
2. Aoki S, Barkovich AJ, Nishimura K, et al. **Neurofibromatosis types 1 and 2: cranial MR findings**. *Radiology* 1989;172:527–34
3. North K. **Neurofibromatosis type 1.** *Am J Med Genet* 2000;97:119–27
4. Menor F, Marti-Bonmati L, Mulas F, et al. **Imaging considerations of central nervous system manifestations in pediatric patients with neurofibromatosis type 1.** *Pediatr Radiol* 1991;21:389–94
5. DiPaolo DP, Zimmerman RA, Rorke LB, et al. **Neurofibromatosis type I: pathologic substrate of high-signal-intensity foci in the brain.** *Radiology* 1995;195:721–24
6. Mori H, Abe O, Okubo T, et al. **Diffusion property in a hamartomatous lesion of neurofibromatosis type 1.** *J Comput Assist Tomogr* 2001;25:537–39
7. Eastwood JD, Fiorella DJ, MacFall JF, et al. **Increased brain apparent diffusion coefficient in children with neurofibromatosis type 1.** *Radiology* 2001;219:354–58
8. Alkan A, Sigirci A, Kutlu R, et al. **Neurofibromatosis type 1: diffusion weighted imaging findings of brain.** *Eur J Radiol* 2005;56:229–34. Epub 2005 Jun 15
9. Tognini G, Ferrozzi F, Garlaschi G, et al. **Brain apparent diffusion coefficient evaluation in pediatric patients with neurofibromatosis type 1.** *J Comput Assist Tomogr* 2005;29:298–304
10. Beaulieu C. **The basis of anisotropic water diffusion in the nervous system: a technical review.** *NMR Biomed* 2002;15:435–55
11. Le Bihan D, Van Zijl P. **From diffusion coefficient to the diffusion tensor.** *NMR Biomed* 2002;15:431–34
12. Song S, Sun S, Ramsbottom MJ, et al. **Dysmyelination revealed through MRI as increased radial (but unchanged axial) diffusion of water.** *Neuroimage* 2002;17:1429–36
13. Song S, Yoshino J, Le TQ, et al. **Demyelination increases radial diffusivity in corpus callosum of mouse brain.** *Neuroimage* 2005;26:132–40
14. Zamboni SL, Loenneker T, Boltshauser E, et al. **Contribution of diffusion tensor MR imaging in detecting cerebral microstructural changes in adults with neurofibromatosis type 1.** *AJNR Am J Neuroradiol* 2007;28:773–76
15. Gill DS, Hyman SL, Steinberg A, et al. **Age-related findings on MRI in neurofibromatosis type 1.** *Pediatr Radiol* 2006;36:1048–56. Epub 2006 Aug 16.
16. **Neurofibromatosis.** *Natl Inst Health Consens Dev Conf Consens Statement.* 1987;6:1–7
17. Basser PJ, Mattiello J, Le Bihan D. **Estimation of the effective self-diffusion tensor from the NMR spin echo**. *J Magn Reson B* 1994;103:247–54
18. Conturo TE, McKinstry RC, Akbudak E, et al. **Encoding of anisotropic diffusion with tetrahedral gradients: a general mathematical diffusion formalism and experimental results.** *J Magn Reson Med* 1996;35:399–412
19. Neil JJ, Shiran SI, McKinstry RC, et al. **Normal brain in human newborns: apparent diffusion coefficient and diffusion anisotropy measured by using diffusion tensor MR imaging.** *Radiology* 1998;209:57–66
20. Szafer A, Zhong J, Anderson AW, et al. **Diffusion-weighted imaging in tissues: theoretical models.** *NMR Biomed* 1995;8:289–96
21. Basser PJ, Jones DK. **Diffusion-tensor MRI : theory, experimental design and data analysis—a technical review.** *NMR Biomed* 2002;15:457–67
22. Wang PY, Kaufmann WE, Koth CW, et al. **Thalamic involvement in neurofibromatosis type 1: evaluation with proton magnetic resonance spectroscopic imaging.** *Ann Neurol* 2000;47:477–84
23. Van Pul C, Buijs J, Janssen MJ, et al. **Selecting the best index for following the temporal evolution of apparent diffusion coefficient and diffusion anisotropy after hypoxic-ischemic white matter injury in neonates.** *AJNR Am J Neuroradiol* 2005;26:469–81
24. Shimony JS, McKinstry RC, Akbudak E, et al. **Quantitative diffusion-tensor anisotropy brain MR imaging: normative human data and anatomic analysis.** *Radiology* 1999;212:770–84
25. Bonekamp D, Nagae LM, Degaonkar M, et al. **Diffusion tensor imaging in children and adolescents: reproducibility, hemispheric, and age-related differences.** *Neuroimage* 2007;34:733–42
26. Ono J, Harada K, Mano T, et al. **Differentiation of dys- and demyelination using diffusional anisotropy.** *Pediatr Radiol* 1997;16:63–66
27. Takahashi M, Ono J, Harada K, et al. **Diffusional anisotropy in cranial nerves with maturation: quantitative evaluation with diffusion MR imaging in rats.** *Radiology* 2000;216:881–85
28. Nair G, Tanahashi Y, Low HP, et al. **Myelination and long diffusion times alter diffusion-tensor-imaging contrast in myelin-deficient shiverer mice.** *Neuroimage* 2005;28:165–74. Epub 2005 Jul 14
29. Mukherjee P, Miller JH, Shimony JS, et al. **Diffusion-tensor MR imaging of gray and white matter development during normal human brain maturation.** *AJNR Am J Neuroradiol* 2002;23:1445–56